RNA-directed off/on switch of RNase H activity using boronic ester formation

Maëva Reverte,[a] Ivan Barvik,[b] Jean-Jacques Vasseur [a] and Michael Smietana*,[a]

[a] *Institut des Biomolecules Max Mousseron, IBMM UMR 5247 CNRS, Université de Montpellier, ENSCM, place Eugène Bataillon, 34095 Montpellier, France. E-mail address: michael.smietana@umontpellier.fr*
[b] *Institute of Physics, Faculty of Mathematics and Physics, Charles University, Ke Karlovu 5, 121 16 Prague 2 (Czech Republic)*

Table of Contents

A) Synthesis of oligonucleotides

Non-modified and 6FAM-labeled sequences were purchased from Eurogentec (Belgium). **ODN1**, **ODN4** and **ODN5** were synthezised on ABI model 394 DNA/RNA synthesizer on 1 µmol scale on commercial long chain alkylamine (LCAA) controlled-pore glass (CPG) as solid support. Oligonucleotides were assembled in TWIST^{TM} synthesis columns (Glen research). BHQ-1 3'CPG was purchased from Link Technologies.

Syntheses were performed in 1 µmol scale using ABI 381A DNA synthesizer by phosphoramidite chemistry with conditions described in Table S1. dTbn-phosphoramidite was synthesized and incorporated at the 5'-end of an oligonucleotide according to previous records.[1,2]

Table S1. Oligonucleotides automated DNA synthesis conditions.

Step	Reaction	Reagent	Time (s)
1	Deblocking	3% TCA in DCM	35
2	Coupling	0.1M amidite in CH_3CN + 0.3M BMT in CH_3CN	180
3	Capping	Ac_2O/THF/Pyridine + 10% NMI in THF	8
4	Oxidation	0.1M I_2 in THF/H_2O/Pyridine	15

After DNA elongation using commercially available phosphoramidites (Chemgenes), the solid support, the cyanoethyl groups and the protecting groups were treated with a solution of a 30% aqueous ammonia at 55°C overnight. The deprotection volume was evaporated, analysed by RP-HPLC, MALDI-TOF MS and finally purified by RP-HPLC.

B) Sequences used in the study

All oligonucleotides synthesized were analyzed by MALDI-TOF MS and the results are presented in the table below (Table S3).

Table S3. MALDI MS of synthesized ODNs.

Name	Sequence (5'-3')	Calcld *m/z* $[M-H]^-$	Obs *m/z* $[M-H]^-$
ODN1	TbnGAATACAAATT	3657.2[a]	3657.6
ODN2	TGAATACAAATT	3651.4	3651.6
ODN3	pTGAATACAAAT	3731.4[a]	3731.8
ODN4	TbnATATTCATCATAG-BHQ1	4795.7	4794.9
ODN5	TbnTGGTTTTGGA-BHQ1	3953.3[a]	3952.3
ORN1	(UUUGUAUUCAGCCCAUAUCUU)	6531.8	6532.1
ORN2	(GAUAUGGGC)	2893.8	2892.9
ORN3	(6FAM-CUAUGAUGAAUAUAGAUACAGAAGCGUCAU)	10167.4	10168.4
ORN4	(6FAM-CUAUGAUGAAUAUAUAUACAGAAGCGUCAU)	10128.3	10127.2
ORN5	(6FAM-CUAUGAUGAAUAUAAAUACAGAAGCGUCAU)	10151.4	10152.8
ORN6	(6FAM-CUAUGAUGAAUAUACAUACAGAAGCGUCAU)	10127.3	10128.1
ORN7	(UUCUGUAU)	2447.5	2448.1
ORN8	(UUCUGUAUp)	2525.4	2525.1
ORN9	(GGC)	932.6	932.0
ORN10	(GAC)	916.6	915.1
ORN11	(GCC)	892.6	891.6
ORN12	(GUC)	893.6	892.8
ORN13	(6FAM-UCCAAAACCAAGGAGGGAG)	6927.8	6926.6
ORN14	(6FAM-UCCAAAACCAAGAAGGGAG)	6911.8	6910.3
ORN15	(UCC)	853.6	852.8

[a] 5'Tbn derivatives are always detected as $[(M-2H_2O)+H]^+$.[1] RNA residues are represented in brakets

HPLC Chromatograms of synthesized sequences

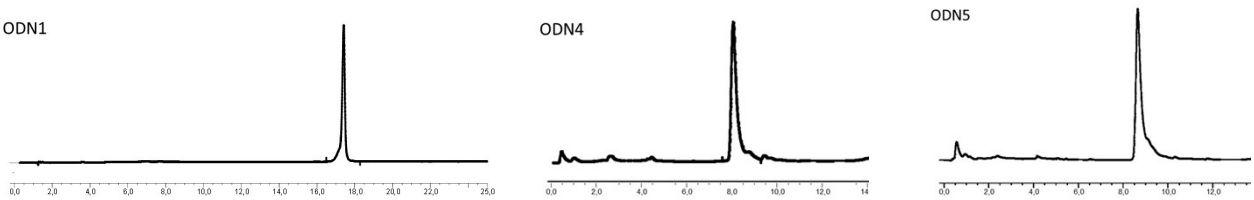

C) RNase H experiments

For all RNase H experiments, aliquots were removed at different time points, heated to 90°C for 20 min to stop enzymatic activity and then analysed by MALDI-TOF MS, RP-HPLC and PAGE. Half-lives were monitored by RP-HPLC and determined by the loss of 50% of the full-length ODN.
In a typical experiment, 1 µL of 0.2 mM of each partner in RNase H reaction buffer (50 mM Tris-HCl, 75 mM KCl, 3 mM $MgCl_2$, 10 mM DTT, final volume 100 µL; pH 8.5) was mixed with 10 U of the enzyme (New England Biolabs) and incubated at 37°.

Figure S1. Graph showing % of the remaining **ORN1** hybridized with **ODN1** when incubated with RNase H

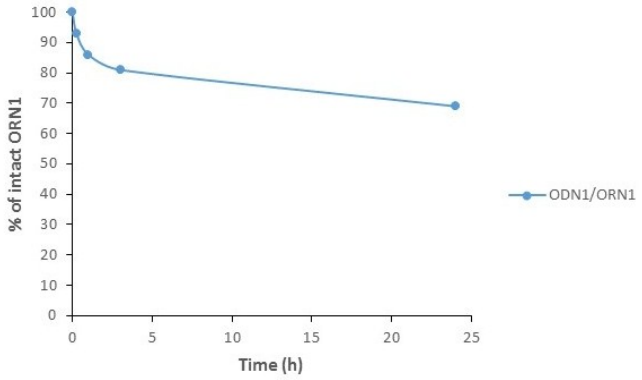

D) Fluorescence experiments

Figure S2. Control experiments in the presence of RNAse H and in the absence of fructose showed no loss of quenching activities over a period of 5h.

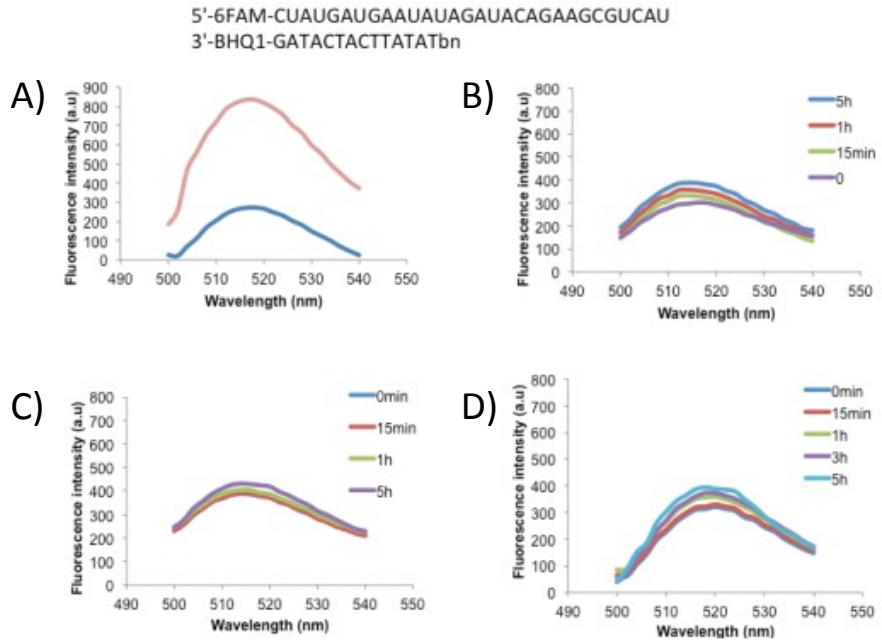

A) Fluorescence spectra of **ORN3** (2 µM) before (red) and after (blue) the addition of **ODN4** (2 µM) at 498nm. B) Fluorescence spectra of duplex **ORN3**/**ODN4** (2 µM of each probe) at 37°C at different times. C) Fluorescence spectra of duplex **ORN3**/**ODN4** (2 µM of each probe) in the presence of fructose (10 mM) and without RNase H at 37°C and at different times. D) Fluorescence spectra of duplex **ORN3**/**ODN4** (2 µM of each probe) in the presence of RNase H (10U) and without fructose at 37°C and at different times.

Figure S3. Graph showing % of the remaining **ORN3** hybridized with **ODN4** (2 µM each) when subjected to RNase H in the presence of varying concentrations of fructose fructose at 37°C.

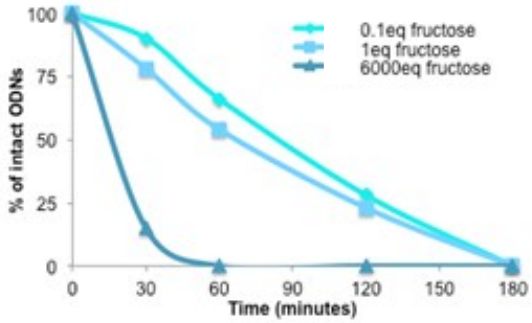

Figure S4. Fluorescence intensity changes upon RNase H-activated cleavage of **ORN3**-**ORN6** (2 µM) by incoming ribonucleoside (100 mM) in the presence of a) **ORN8** a 3'-phosphate ended helper and b) **ONR7** a 3'-OH ended helper at pH 8.5 after 60 min of incubation. λex = 498nm, λem = 518nm (Ex slit : 5.0; Em slit : 10.0).

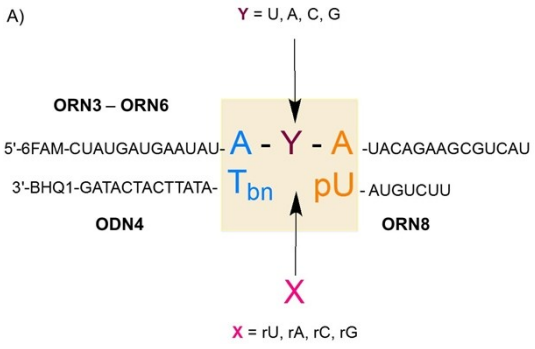

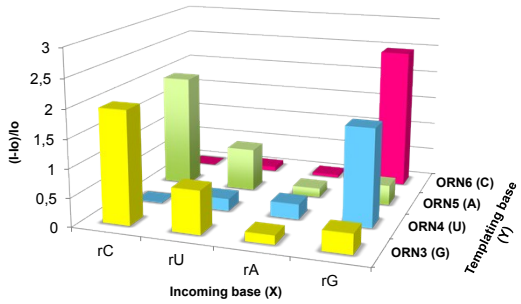

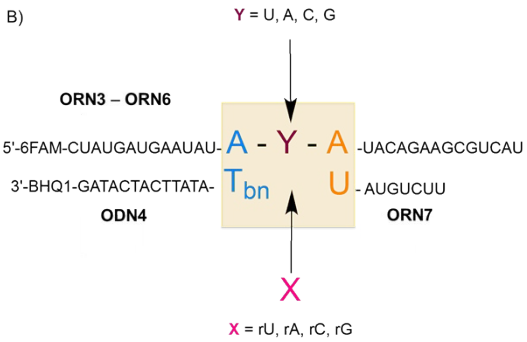

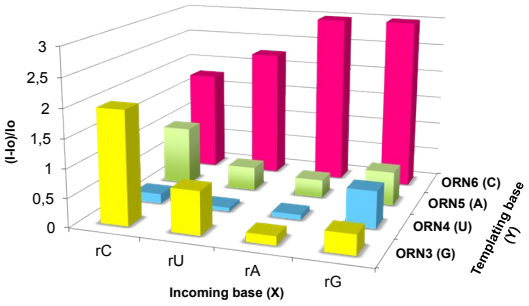

Figure S5. Fluorescence intensity changes upon RNase H-activated cleavage of **ORN3**-**ORN6** (2 µM) by incoming ribonucleotide (100 mM) in the presence of a) **ORN8** a 3'-phosphate ended helper and b) **ONR7** a 3'-OH ended helper at pH 8.5 after 15 and 60 min of incubation. λex = 498nm, λem = 518nm (Ex slit : 5.0; Em slit : 10.0).

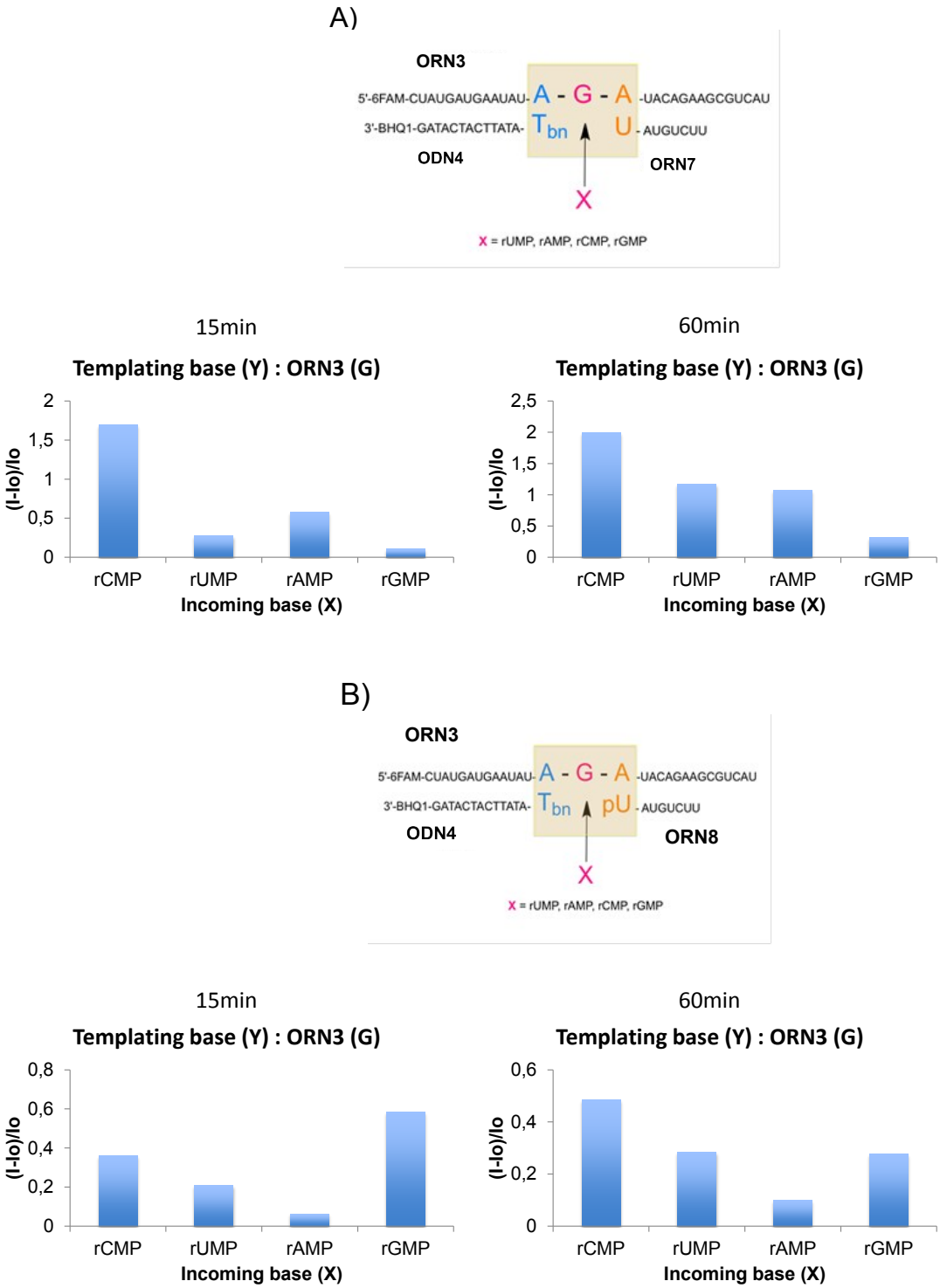

E) Figure S6: Time courses degradations analysed by RP-HPLC of **ORN13** and **ORN14** upon RNase H-activated cleavage in presence of **ODN5** (2 µM) et ORN15 (2 µM)

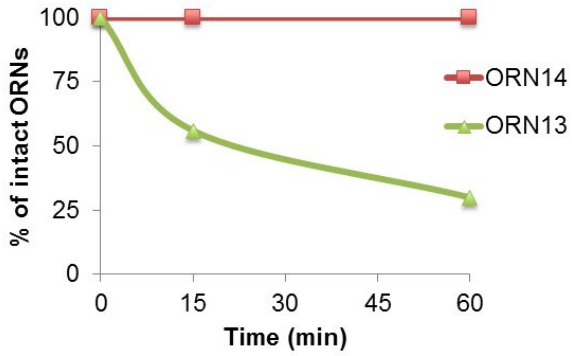

F) Figure S7. Difference in fluorescence intensity between **ORN13** and **ORN14** against RNA concentration. λex = 498nm, λem = 518nm (Ex slit : 5.0; Em slit : 10.0).

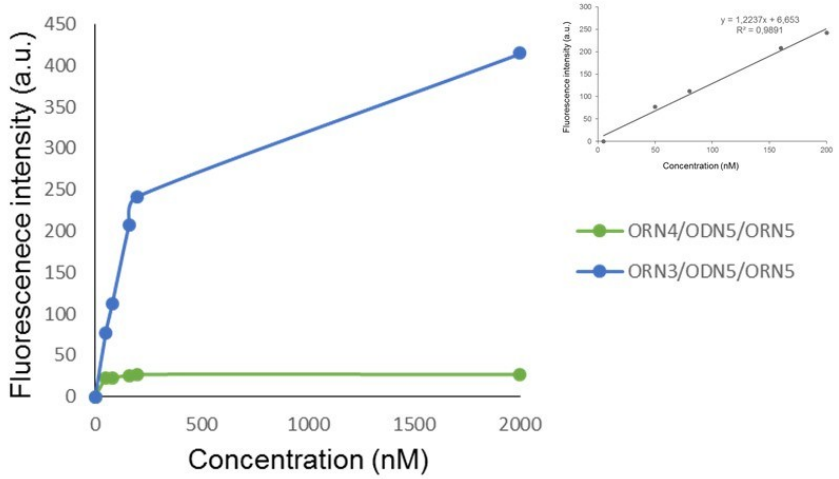

Data were recorded as mean ± standard deviation based on three independent measurements. The linear response range was determined and used to derive LOD. The LOD was calculated based on the standard deviation of the response of y-intercept (SD) and the slope of the calibration curve (S) according to the formula: LOD = 3.3 (SD/S). The values of SD and slope was obtained from the LINEST function by creating a calibration curve in Microsoft Excel.

Table S4. Determination of LOD

Time (min)	Linearity range (nM)	Slope	SD (slope)	y-intercept	SD (y-intercept)	Regression coefficient	LOD (nM)
15	5-200	1.22	0.07	6.65	9.06	0,99	24.5

G) Molecular Dynamics

The simulated system (complex of *E. coli* RNase H and rA10*dT5) was derived from our previous models[3] that were based on the 1RDD crystal structure of *E. coli* RNase H.[4] The crystal structure of Human RNase H[5] enabled to position the second magnesium ion into the *E. coli* RNase H active site in our models.[3b] Here, dT10 was shortened to dT5 and the boronic moiety was added on its 5'-end. The boronic group was modeled by means of the *Molefacture* plugin from the VMD 1.9.3 software package.[6] The CHARMM force field[7] was used for *E. coli* RNase H and for both nucleic acids. The nucleotide with the boronic group (as well as modified side chains of Lys99 and Thr43 amino acids lacking one hydrogen atom) were parametrized using the *ParamChem* web server (https://cgenff.paramchem.org/).[8] Finally, biomolecules were surrounded by TIP3P water molecules.[9] MD trajectories were produced using the NAMD 2.12 software package (11) by means of the NVIDIA graphical processing units. Binding of the boronic group toward modified side chains of Lys99 and Thr43 was modeled by means of additional extraBonds that are implemented in the NAMD 2.12 software package.[10] The smooth Particle-mesh Ewald (PME) method was employed for long-range electrostatic forces.[11] The non-bonded cutoff was set to 12 Å. The SHAKE algorithm was applied to constrain bonds where the hydrogen atoms were involved.[12] After reaching the energy minimum of simulated systems, the Langevin dynamics was used for a temperature control with target temperature set to 310 K.[10] The Langevin piston method was applied to reach an efficient pressure control with target pressure set to 1 atm.[10] The integration time step was set to 2 fs. MD simulations lasted for 5 ns. MD trajectories were analyzed with the aid of the VMD software package.[13] Figures were produced by means of the UCSF Chimera software package (https://www.cgl.ucsf.edu/chimera/).

References

1. A. R. Martin, I. Barvik, D. Luvino, M. Smietana and J.-J. Vasseur, *Angew. Chem., Int. Ed.*, 2011, **50**, 4193.
2. A. R. Martin, K. Mohanan, D. Luvino, N. Floquet, C. Baraguey, M. Smietana and J. J. Vasseur, *Org. Biomol. Chem.*, 2009, **7**, 4369.
3. (a) I. Barvik, *Nucleos. Nucleot. Nucl.*, 2005, **24**, 435; (b) H. Sipova, T. Springer, D. Rejman, O. Simak, M. Petrova, P. Novak, S. Rosenbergova, O. Pav, R. Liboska, I. Barvik, J. Stepanek, I. Rosenberg and J. Homola, *Nucleic Acids Res.*, 2014, **42**, 5378.

4. K. Katayanagi, M. Okumura and K. Morikawa, *Proteins-Structure Function and Genetics*, 1993, **17**, 337.
5. M. Nowotny, S. A. Gaidamakov, R. Ghirlando, S. M. Cerritelli, R. J. Crouch and W. Yang, *Molecular Cell*, 2007, **28**, 264.
6. W. Humphrey, A. Dalke and K. Schulten, *Journal of Molecular Graphics & Modelling*, 1996, **14**, 33.
7. K. Vanommeslaeghe and A. D. MacKerell, *Biochim. Biophys. Acta-Gen Subjects*, 2015, **1850**, 861.
8. (a) K. Vanommeslaeghe, E. Hatcher, C. Acharya, S. Kundu, S. Zhong, J. Shim, E. Darian, O. Guvench, P. Lopes, I. Vorobyov and A. D. MacKerell, *J. Comput. Chem.*, 2010, **31**, 671; (b) K. Vanommeslaeghe and A. D. MacKerell, *Journal of Chemical Information and Modeling*, 2012, **52**, 3144; (c) K. Vanommeslaeghe, E. P. Raman and A. D. MacKerell, *Journal of Chemical Information and Modeling*, 2012, **52**, 3155.
9. W. L. Jorgensen, J. Chandrasekhar, J. D. Madura, R. W. Impey and M. L. Klein, *J. Chem. Phys.*, 1983, **79**, 926.
10. J. C. Phillips, R. Braun, W. Wang, J. Gumbart, E. Tajkhorshid, E. Villa, C. Chipot, R. D. Skeel, L. Kale and K. Schulten, *J. Comput. Chem.*, 2005, **26**, 1781.
11. T. E. Cheatham, J. L. Miller, T. Fox, T. A. Darden and P. A. Kollman, *J. Am. Chem. Soc.*, 1995, **117**, 4193.
12. J. P. Ryckaert, G. Ciccotti and H. J. C. Berendsen, *J. Comput. Phys.*, 1977, **23**, 327.
13. D. A. Pearlman, D. A. Case, J. W. Caldwell, W. S. Ross, T. E. Cheatham, S. Debolt, D. Ferguson, G. Seibel and P. Kollman, *Comput. Phys. Commun.*, 1995, **91**, 1.